https://doi.org/10.15407/ujpe66.8.643

F.H. OBEED

Department of Physics, Faculty of Education for Girls, University of Kufa
(Al-Najaf, Iraq; e-mail: fatimahh.alfatlawi@uokufa.edu.iq)

CALCULATION OF NUCLEAR PROPERTIES FOR $^{56-62}$Fe ISOTOPES IN THE MODEL SPACE (HO) USING NuShellX@MSU CODE

The nuclear shell model has been applied to calculate the yrast energy levels, quadrupole transition probability (BE2), deformation parameter β_2, rotational energy ($\hbar w$), and inertia moment ($2\theta/\hbar^2$) for the ground state band. The NuShellX@MSU code has been used to determine the nuclear properties of $^{56-62}$Fe isotopes, by using the harmonic oscillator (HO) model space for $P(1f_{7/2})$, $N(2p_{3/2})$, $N(1f_{5/2})$, and $N(2p_{1/2})$ orbits and (HO) interaction. The results are in good agreement with the available experimental data on the above nuclear properties and all nuclei under study. In addition, the back bending phenomenon has been explained by the calculations, and it has been very clear in ^{58,60,62}Fe nuclei. It has also been confirmed and determined the most spins and parities of energy levels. In these calculations, new values have been theoretically determined for the most nuclear properties which were previously experimentally unknown.

Keywords: yrast energy levels, quadrupole transition probability, NuShellX@MSU code, deformation parameter, rotational frequency, inertia moment.

1. Introduction

The nucleus is a quantum mechanical system that consists of a number of protons and neutrons. The dynamics of the nuclei can be determined by the nucleons moving outside the compact core that consists of valence particles. The accurate knowledge of the interaction among the valence particles is of a fundamental importance for a proper description of the nuclear properties [1]. Several nuclear models have described the nuclear properties of many nuclei, and one of these models is the successful nuclear shell model (NSM), identifying the energy states, their locations, and the transitions between these states, which gives an important description of the nuclei [2, 3]. Among the nuclei, ^{48}Ca magic core plays a central role in theoretical calculations because its maximum number of valence protons in $P(1f_{7/2})$ orbit and valence neutrons in $N(2p_{3/2})$, $N(1f_{5/2})$, and $N(2p_{1/2})$ orbits. The number of active valence particles is low enough in those nuclei, which allows one to get their full shell-model description. Those nuclei can form such interesting structure as an island in the nuclide chart [4]. Many researchers studied the shell model in the f_p region to describe the characteristics of many isotopes related to pf-shell nuclei [5]. It is worth to mention a new shell structure in f_p-shell nuclei [6], the full f_p shell calculation of ^{51}Ca and ^{51}Sc [7], and large-scale shell model calculations for odd-odd $^{58-62}$Mn isotopes [8]. Each isotope of some nucleus has energy levels with properties that may or may not be the same. Depending on the nuclear characteristics of each isotope, the energy levels are very important for the identification of the isotope. Its energy levels (vibrational or rotational) can be divided into different bands. In addition to the ground band and the unstable beta or gamma bands, there is the

yrast band of states with the lowest energy and momentum. The study of this yrast-band is very important for identifying the nuclear properties [9]. It has observed that some nuclei increase their energy levels by increasing the momentum but with different rates, because of the curvature of the inertia moment $\frac{2\theta}{\hbar^2}$ (MeV^{-1}) curve of the emitted gamma energy function. Due to the importance of recognizing the back bending curvature that occurs in the energy levels of some isotopes, many previous studies considered this phenomenon including the nuclear moment of Inertia at high rotational frequencies for ^{158}Dy, ^{160}Dy, ^{162}Er, and ^{168}Yb nuclei [10] and the nuclear moment of inertia at high spin of $^{152-154}$Sm, $^{154-160}$Gd, $^{156-164}$Dy, $^{160-170}$Er, $^{164-174}$Yb, $^{170-180}$Hf, and $^{172-186}$W nuclei [11]. The main aim of the present research is to describe some of the nuclear properties of $^{56-62}$Fe isotopes that have nucleons lying between the magic numbers 20 and 28. We will employ the (HO) interaction in the (HO) model space for ($P(1f_{7/2})$, $N(2p_{3/2})$, $N(1f_{5/2})$, and $N(2p_{1/2})$ orbits. The calculations have been performed by using NuShellX@MSU code.

2. Theory

The studies of yrast energy levels and quadrupole transitions, as well as the quadrupole deformation parameter in the nucleus, are of high importance for understanding the nuclear structure, identifying its positions between different nuclei and the characteristics of the structure to which they belong [11]. Nuclear properties can be described by using the Schrödinger equation for A nucleons. We now consider the general formalism that is used in the effective interaction theory whose purpose, in particular, is to solve the Schrödinger equation for the A-nucleon system [12]:

$$\hat{H}\psi(1,2,...,A) = E\psi(1,2,...,A), \tag{1}$$

where ($\hat{H}$) is the sum representing both the kinetic energy operators of nucleons and two-body interactions between nucleons [13]:

$$\hat{H} = \hat{H}_o + \hat{V}, \tag{2}$$

where $\hat{H}_o$ is the sum of single-particle Hamiltonians, and $\hat{V}$ is a residual interaction. The spherical mean field has been produced by the closed core corresponding to the ($\hat{H}_o$) part, which is a standard phenomenological single-particle potential given by a harmonic oscillator. All valence nucleons outside the closed core interact through the (H_1) part, which is taken into account for describing nuclei by using the specified model space. In the nuclear shell model calculations [14], the effective interactions can be derived from the free NN interaction. They can be also obtained in a more phenomenological manner, by combining the results from the free NN interaction and from the fits of selected experimental data [15]. The Hamiltonian of a nucleus can be formed by the inert core and two orbiting nucleons in the valence shells that can be split into two parts: $H = H_{\mathrm{core}} + H_{12}$. By using the same notations as in Eq. (2) [16], we have

$$H_{\mathrm{core}} = \sum_{k=3}^{A} T(k) + U(k) + \sum_{3=k<1}^{A} V(l,k) - \sum_{k=3}^{A} U(k), \tag{3}$$

$$H_{12} = \sum_{k=1}^{2} T(k) + U(k) + \sum_{k=1}^{2}\sum_{l=3}^{A} V(k,l) + \\ + V(1,2)) - \sum_{k=1}^{2} U(k), \tag{4}$$

H_{core}: expresses the interactions between the core particles (labeled by $k = 3, ..., A$), while H_{12} represents the contribution from for two additional particles. We can write $H_{12}^{(0)} = [T(1)+U(1)]+[T(2)+U(2)]$ including the single-particle kinetic and potential energies of the particles (1 and 2), while $H_{12}^{(1)}$ denotes the residual interaction. We have

$$H_{12} = \sum_{l=3}^{A} V(1,l) + U(1) + \sum_{l=3}^{A} -U(2)V(1,2). \tag{5}$$

The equations above hold for any average field $U(k)$. For $U(k) = \sum_{l=3}^{A} V(k,l)$, the equation take the form

$$H_{12} = V(1,2). \tag{6}$$

If the only two-particle term $V(1,2)$ remains in Eq. (5), the information about the properties of the NN interaction $V(k,l)$ can be obtained by analyzing the contribution of the two particles to the total energy of a nucleus that consists of an inert closed core plus two nucleons [17]. The model space and effective interaction are essential inputs for calculating the energy levels, the electric quadrupole probability, and another nuclear properties like the electric

quadrupole deformation, inertial moment, and rotational energy. The electric matrix element between the initial and final nuclear states can be written as

$$M(EJ) = \left\langle J_f \| \sum_k e(k)\hat{Q}_J(\mathbf{r})_k \| J_i \right\rangle_{MS}, \quad (7)$$

where $e(k)$ is the electric charge for the k-th nucleon, and $e(k) = 0$ for a neutron. By adding a valence neutron, we will induce the polarization of the core into configurations outside the adopted model space. In this case, the reduced electric matrix element will be written in terms of the proton and neutron as follows:

$$M(EJ) = \sum t_z e(t_z) \langle J_f \| \hat{Q}_J(\mathbf{r}, t_z) \| J_i \rangle, \quad (8)$$

where $\langle J_f \| \hat{Q}_J(\mathbf{r}, t_z) \| J_i \rangle$ is expressed as the sum of the products of the one-body density matrix (OBDM) times the single-particle matrix elements:

$$\langle J_f \| \hat{Q}_J(\mathbf{r}, t_z) \| J_i \rangle =$$

$$= \sum jj^{'} OBDM(Ji, Jf, J, t_z, j, j^{'}) j^{'} \langle j^{'} \| O^J(\mathbf{r}, t_z) \| j \rangle, \quad (9)$$

where j and $j^{'}$ denote single-particle states for the shell model space. By assigning effective charges $e_{\text{eff}}(t_z)$ to the protons and neutrons which are outside of the closed shell, the matrix element can be written in terms of effective charges by using the equation

$$M(EJ) = \sum_{t_z} e_{\text{eff}}(t_z) \langle Jf \| \hat{Q}_2(\mathbf{r}, t_z) \| Ji \rangle_{MS}, \quad (10)$$

$e_{\text{eff}}(t_z)$ represents the effective charge for a nucleon which can be written as

$$e_{\text{eff}}(t_z) \langle J_f \| (\hat{Q}(\mathbf{r}, t_z) \| J_i \rangle_{MS} =$$

$$= e(t_z \langle J_f \| (\hat{Q}(\mathbf{r}, t_z) \| J_i \rangle_{MS} + \langle J_f \| (\hat{\Delta Q})(\mathbf{r}, t_z) \| J_i \rangle_{CP}. \quad (11)$$

Hence, we get

$$e_{\text{eff}}(t_z) = e(t_z) + \frac{\langle J_f \| (\hat{\Delta Q})(\mathbf{r}, t_z) \| J_i \rangle_{CP}}{\langle J_f \| \hat{Q}(\mathbf{r}, t_z) \| J_i \rangle_{MS}} =$$

$$= \{e(t_z) + e\delta e(t_z)\}, \quad (12)$$

$\delta e(t_Z)$ is expressed from the polarization charge for a nucleon. From relation (12), it is seen that the difference between the effective charge and the charge of a single nucleon is referred to the polarization charge. The effective charge values have been deduced from the observed static and transition moments. It is explained that the value may depend somewhat on the orbit of the nucleon. Especially, the polarization effect decreases, when the binding energy of nucleons becomes low, since the nucleon is outside the nuclear surface, and the effectiveness of polarizing the core is less:

$$B(EJ) = \frac{|M(EJ)|^2}{(2Ji + 1)}. \quad (13)$$

The state $J = 2,\ M = 0 >$ for $J_{[i]} = J_f$ is defined for the electric quadrupole moment according to the equation:

$$Q(J = 2) = \begin{pmatrix} J_i & J & J_i \\ -J_i & J & J_i \end{pmatrix} \frac{\sqrt{16\pi}}{5} M(EJ). \quad (14)$$

The intrinsic quadrupole moment (Q_0) can be determined from the reduced transition probability $B(E2)$ as [18]:

$$B(E2\colon J_i, \quad k \to J_f, k) = \frac{5}{16\pi} Q_0^2 \langle J_i k; 20 | J_f \rangle^2, \quad (15)$$

$\langle J_i k; 20 \mid J_f \rangle$ is a Clebsch–Gordan coefficient that governs the coupling of the angular momenta. For the electromagnetic transitions between the states $J_i = J$ and $J_f = J + 2$, with $k = 0$, the Clebsch–Gordan coefficient in (15) can be rewritten as [19]:

$$\langle J0\ k; 20 | (J + 2)0 \rangle^2 = \frac{(3(J + 1)(J + 2))}{(2(2J + 1)(2J + 3))}. \quad (16)$$

Hence, from the reduced electric quadrupole transition probability, $B(E2) \uparrow$, from the spin 0^+ ground state to the first excited spin 2^+ state, we can calculate the values of the intrinsic quadrupole moment Q_0 according to the following relation:

$$Q_0 = \sqrt{\frac{16\pi}{5} \times B(E2 \uparrow)}. \quad (17)$$

We note that the electromagnetic excitation $B(E2) \uparrow$ and decay $B(E2) \downarrow$ of a nuclear state are related by the relation:

$$B(E2\colon J_f \to J_i) = \left(\frac{(2J_i + 1)}{(2J_f + 1)}\right) B(E2\colon J_i \to J_f). \quad (18)$$

The electric quadrupole deformation parameter can be calculated by the reduced transition probability $B(E2 \uparrow)$ defined as [20]:

$$\beta_2 = \frac{4\pi}{3ZR_0^2} \times \sqrt{BE2 \uparrow; (0_1^+ \to 2_1^+)}, \quad (19)$$

Table 1. **Comparison between theoretical and experimental excitation energies (MeV) for $^{56-62}$Fe (even-even) nuclei**

Nuclei	Theoretical values		Experimental values	
	Yrast levels	Energies (MeV)	Yrast levels	Energies (MeV) [26]
^{56}Fe	0_1^+	0	0^+	0
	2_1^+	0.814	2^+	0.846
	4_1^+	2.077	4^+	2.085
	6_1^+	3.655	6^+	3.388
	8_1^+	5.458	8^+	5.255
	10_1^+	8.100	$10^{(+)}$	7.820
Nuclei	Yrast levels	Energies (MeV)	Yrast levels	Energies (MeV) [27]
^{58}Fe	0_1^+	0	0^+	0
	2_1^+	0.887	2^+	0.811
	4_1^+	2.141	4^+	2.076
	6_1^+	3.668	6^+	3.596
	8_1^+	5.047	8^+	5.343
	10_1^+	7.418	(10^+)	7.242
	12_1^+	9.947	(12)	9.984
Nuclei	Yrast levels	Energies (MeV)	Yrast levels	Energies (MeV) [28]
^{60}Fe	0_1^+	0	0^+	0
	2_1^+	0.932	2^+	0.824
	4_1^+	2.309	4^+	2.114
	6_1^+	3.998	(6^+)	3.582
	8_1^+	5.639	8^+	5.333
	10_1^+	7.038	10^+	6.475
	12_1^+	8.918	–	8.920
Nuclei	Yrast levels	Energies (MeV)	Yrast levels	Energies (MeV) [29]
^{62}Fe	0_1^+	0	0^+	0
	2_1^+	1.028	2^+	0.877
	4_1^+	2.344	(4^+)	2.176
	6_1^+	4.032	$(2^+, 3^+, 4^+)$	4.050
	8_1^+	5.928	–	5.474
	10_1^+	7.278	–	–
	12_1^+	9.406	–	–

Z is the atomic number, and $R_0^2 = 0.0144A^{(2/3)}(b)$. But the static electric quadrupole moment Q values are determined by the intrinsic moment Q_0 in the laboratory reference system from the equation [21]:

$$Q = Q_0 \left\{ \frac{(3K^2 - I(I+1)}{((I+1)(2I+3))} \right\}, \tag{20}$$

I expresses the spin of the state member of the rotational band for the ground state, and K is its projection on the symmetry axis. In some nuclei, there is a sudden change in the inertial momentum value at a relatively high total angular momentum values leading to a decrease in the rotational energy $\hbar w$ (MeV) of the nucleus at that total angular momentum. This leads to the back-bending in the energy curve with the total angular momentum [22]. When the relation between inertial moment $2\theta/\hbar^2$ (MeV^{-1}) and the rotational energy $\hbar w$) (MeV) appears, the change with Z is clearly inverted [23]. The inertial moment can be calculated by the difference in the energies of two levels in the yrast rotational bands of statesaccording

to the relation [24]:

$$2\theta/\hbar^2 = \frac{4J-2}{E(J)-E(J-2)} = \frac{4J-2}{E_y}. \quad (21)$$

In addition, the rotational energy resulting from the transition from a state with angular momentum (J) to a lower state with angular momentum $(J-2)$ can be calculated according to the relation.

$$\hbar w = \frac{E(J)-E(J-1)}{\sqrt{J(J+1)}-\sqrt{(J-2)(J-1)}}. \quad (22)$$

3. Results and Discussion

The yrast band structure for $^{56-62}$Fe isotopes has been explained by employing the (HO) model space and (HO) interaction in NuShellX@MSU code which represents a set of programs for carrying out nuclear shell-model calculations. This code can be used as a set of computer codes written by Rae and enables one to obtain exact energies, eigenvectors, and spectroscopic overlaps for low-lying states in the shell-model Hamiltonian matrix calculations with very large basis dimensions. It uses a J-coupled proton-neutron basis and J-scheme matrix dimensions up to the order of 100 million [25]. In this paper, we will explain that the nuclear shell model provides one of the most established ways to describe atomic nucleus properties with low or medium masses such as $^{56-62}$Fe nuclei that are a part of both $1f_{7/2}$ and f_p-shells formed of the four single-particle orbitals which are $(1f_{7/2})$ for six protons and, $(2p_{3/2}\&1f_{5/2})$ as well as $(2p_{1/2})$ for two, four, six, and eight neutrons, respectively, outside the ^{48}Ca double shell closure. Each valence nucleon orbit provides positive-parity states for energy levels of all possible mixing configurations. In this work, the energy levels for the ground bands, electric quadrupole transition probability $(BE2)$, deformation parameter (β_2), rotational energy $(\hbar w)$, and inertia moment $(2\theta/\hbar^2)$ have been calculated. On the other hand, the relationship between the moment of inertia and the rotational energy of all nuclei has been drawn, which has explained the back bending appearance in most nuclei. Now, $^{56-62}$Fe nuclei will be discussed in what follows.

3.1. Energy levels

Table 1 shows the comparison between the expected theoretical and the experimental values for the positive parity states of all $^{56-62}$Fe nuclei, which has been achieved by employing the (HO) interaction with NuShellX@MSU code. ^{56}Fe nucleus ground state is composed of six protons and two neutrons outside the ^{48}Ca double shell closure which occupy the $(1f_{7/2})$ shell for protons and $(2p_{3/2}, 1f_{5/2}$, and $2p_{1/2})$ orbits for neutrons. For this nucleus, the comparison shows the excellent agreement between the predicted theoretical results of calculations such as $(0;0^+)$, $(0.814;2^+)$, $(2.077;4^+)$, $(3.655;6^+)$, $(5.458;8^+)$, and $(8.100;10^+)$ MeV and experimental data $(0;0^+)$, $(0.846;2^+)$, $(2.085;4^+)$, $(3.388;6^+)$, $(5.255;8^+)$ and $(7.820;10^+)$ MeV for the yrast band. For the experimental level 7.820 MeV, we have confirmed parity $(+)$. The available experimental data on ^{56}Fe nucleus have been taken from Refs. [26]. We note that ^{58}Fe nucleus has six protons and four neutrons above ^{48}Ca closed core. The comparison shows that the expected theoretical values for energies $0.887, 2.141, 3.668$ and 5.04 MeV have been better correspond with experimental energies [27] at values $0.811, 2.076, 3.596$ and 5.343 MeV at same spins $(0^+, 2^+, 4^+, 6^+$ and $8^+)$ respectively. But though the experimental energy value 7.242 MeV agrees with the theory, the theoretical spin and parity 10^+ were unconfirmed experimentally. Moreover, the parity $(+)$ and calculated spin (12) are confirmed for the experimental energy level 9.984 MeV. In the case of ^{60}Fe isotope, there are six protons and six neutrons distributed on $1f_{7/2}(p)$ shell and $(2p_{3/2}(n)$, $1f_{5/2}(n)$, and $2p_{1/2}(n)$ orbits over ^{48}Ca closed core. The experimental data [28], namely, $(0;0^+)$, $(0.824;2^+)$, $(2.114;4^+)$, $(5.333;8^+)$, and $(6.475;10^+)$ MeV have been compared with the theoretical values, by showing a sufficient agreement. An experimental level of 3.582 MeV has been affirmed except for the spin

Table 2. **Skyrme20 (SK20) parameters values**

Parameters	Values
t_0	-1445.322
t_1	264.867
t_2	-131.786
t_3	12103.863
w_0	148.637
a	0.5
x_0	0.340
x_1	0.580
x_2	0.127
x_3	0.030

Table 3. **Comparison between theoretical and experimental values of the electric quadrupole transition, intrinsic moment, and quadrupole deformation for $^{56-62}$Fe (even-even)nuclei**

Nuclei	$J_i \to J_f$	$(BE2)_{\text{theor.}}$ (e^2 fm^4)	$(BE2)_{\text{exp.}}$(e^2 fm^4) [26]	$(\beta_2)_{\text{theor.}}$	$(\beta_2)_{\text{exp.}}$ [26]	$(Q_0)_{\text{theor.}}(b)$	$(Q_0)_{\text{exp.}}(b)$ [26]
^{56}Fe		$e_p = 1.5663e$ $e_n = 0.894e$		0.250	0.250 ± 5	1.037	1.366
	$2_1^+ \to 0_1^+$	214.2	213.9 ± 89				
	$4_1^+ \to 2_1^+$	286.4	305.5 ± 64				
	$6_1^+ \to 4_1^+$	104.2	509 ± 51				
	$8_1^+ \to 6_1^+$	65.02	51 ± 76				
	$10_1^+ \to 8_1^+$	38.93	–				
Nuclei	$J_i \to J_f$	$(BE2)_{\text{theor.}}$ (e^2 fm^4)	$(BE2)_{\text{exp.}}$ (e^2 fm^4) [27]	$(\beta_2)_{\text{theor.}}$	$(\beta_2)_{\text{exp.}}$ [27]	$(Q_0)_{\text{theor.}}(b)$	$(Q_0)_{\text{exp.}}(b)$ [27]
^{58}Fe		$e_p = 1.391e$ $e_n = 0.886e$		0.262	0.262 ± 4	1.1139	1.1135
	$2_1^+ \to 0_1^+$	247.1	246.8 ± 80				
	$4_1^+ \to 2_1^+$	301.8	627.1 ± 93				
	$6_1^+ \to 4_1^+$	275.3	346.9 ± 133				
	$8_1^+ \to 6_1^+$	48.93	18.67 ± 53				
	$10_1^+ \to 8_1^+$	27.86	–				
	$12_1^+ \to 10_1^+$	19.50	–				
Nuclei	$J_i \to J_f$	$(BE2)_{\text{theor.}}$ (e^2 fm^4)	$(BE2)_{\text{exp.}}$ (e^2 fm^4) [28]	$(\beta_2)_{\text{theor.}}$	$(\beta_2)_{\text{exp.}}$ [28]	$(Q_0)_{\text{theor.}}(b)$	$(Q_0)_{\text{exp.}}(b)$ [28]
^{60}Fe		$e_p = 1.5663e$ $e_n = 0.894e$		0.224	0.224 ± 11	0.977	0.9766
	$2_1^+ \to 0_1^+$	190.1	189.85 ± 196				
	$4_1^+ \to 2_1^+$	239.8	195.4 ± 55				
	$6_1^+ \to 4_1^+$	131.4	–				
	$8_1^+ \to 6_1^+$	46.03	–				
	$10_1^+ \to 8_1^+$	16.90	–				
	$12_1^+ \to 10_1^+$	4.394	–				
Nuclei	$J_i \to J_f$	$(BE2)_{\text{theor.}}$ (e^2 fm^4)	$(BE2)_{\text{exp.}}$ (e^2 fm^4) [29]	$(\beta_2)_{\text{theor.}}$	$(\beta_2)_{\text{exp.}}$ [29]	$(Q_0)_{\text{theor.}}(b)$	$(Q_0)_{\text{exp.}}(b)$ [29]
^{62}Fe		$e_p = 1.5663e$ $e_n = 0.894e$		0.2289	0.229 ± 13	1.0168	1.0163
	$2_1^+ \to 0_1^+$	205.7	205.6 ± 233				
	$4_1^+ \to 2_1^+$	236.6	–				
	$6_1^+ \to 4_1^+$	121	–				
	$8_1^+ \to 6_1^+$	119.2	–				
	$10_1^+ \to 8_1^+$	23.42	–				
	$12_1^+ \to 10_1^+$	0.3789	–				

and parity (6^+). The (12^+) state have been determined for an experimental level of 8.920 MeV with the spin and parity unknown experimentally. Finally, ^{62}Fe isotope has six proton and eight neutrons situated at $1f_{7/2}(p)$ shell and $2p_{3/2}(n)$, $1f_{5/2}(n)$, and $2p_{1/2}(n)$ orbits over ^{48}Ca closed core. For ^{62}Fe nucleus, we have got agreement for theoretical values $(0; 0^+)$ and $(1.028, 2^+)$ with experimental values

Table 4. **Comparison between theoretical and experimental values of the gamma energies, rotation frequency, and inertia moment for $^{56-62}$Fe (even-even) nuclei**

Nuclei	$J_i \to J_f$	Theoretical values			Experimental values		
		Gamma energies, MeV	$\hbar w$, MeV	$2\frac{\theta}{\hbar^2}$, MeV^{-1}	Gamma energies, MeV [26]	$\hbar w$, MeV [26]	$2\frac{\theta}{\hbar^2}$, MeV^{-1} [26]
^{56}Fe	$2_1^+ \to 0_1^+$	0.814	0.332	7.371	0.846	0.345	7.092
	$4_1^+ \to 2_1^+$	1.263	0.624	11.085	1.239	0.613	11.299
	$6_1^+ \to 4_1^+$	1.578	0.785	13.941	1.303	0.648	16.884
	$8_1^+ \to 6_1^+$	1.803	0.899	16.638	1.867	0.931	16.68
	$10_1^+ \to 8_1^+$	2.642	1.319	14.383	2.565	1.280	14.814
Nuclei	$J_i \to J_f$	Gamma energies, MeV	$\hbar w$, MeV	$2\frac{\theta}{\hbar^2}$, MeV^{-1}	Gamma energies, MeV [27]	$\hbar w$, MeV [27]	$2\frac{\theta}{\hbar^2}$, MeV^{-1} [27]
^{58}Fe	$2_1^+ \to 0_1^+$	0.887	0.362	6.764	0.811	0.331	7.398
	$4_1^+ \to 2_1^+$	1.254	0.619	11.164	1.265	0.625	11.067
	$6_1^+ \to 4_1^+$	1.527	0.760	14.407	1.52	0.756	14.473
	$8_1^+ \to 6_1^+$	1.379	0.687	21.754	1.747	0.871	17.172
	$10_1^+ \to 8_1^+$	2.371	1.184	16.026	1.899	0.948	20.011
	$10_1^+ \to 8_1^+$	2.529	1.263	18.189	2.742	1.369	16.776
Nuclei	$J_i \to J_f$	Gamma energies, MeV	$\hbar w$, MeV	$2\frac{\theta}{\hbar^2}$, MeV^{-1}	Gamma energies, MeV [28]	$\hbar w$, MeV [28]	$2\frac{\theta}{\hbar^2}$, MeV^{-1} [28]
^{60}Fe	$2_1^+ \to 0_1^+$	0.932	0.380	6.438	0.824	0.336	7.281
	$4_1^+ \to 2_1^+$	1.377	0.680	10.167	1.29	0.637	10.853
	$6_1^+ \to 4_1^+$	1.689	0.840	13.025	1.468	0.730	14.986
	$8_1^+ \to 6_1^+$	1.641	0.818	18.281	1.751	0.873	17.133
	$10_1^+ \to 8_1^+$	1.399	0.698	27.162	1.142	0.570	33.274
	$12_1^+ \to 10_1^+$	1.88	0.939	24.46	2.445	1.221	18.814
Nuclei	$J_i \to J_f$	Gamma energies, MeV	$\hbar w$, MeV	$2\frac{\theta}{\hbar^2}$, MeV^{-1}	Gamma energies, MeV [29]	$\hbar w$, MeV [29]	$2\frac{\theta}{\hbar^2}$, MeV^{-1} [29]
^{62}Fe	$2_1^+ \to 0_1^+$	1.028	0.419	5.836	0.877	0.358	6.841
	$4_1^+ \to 2_1^+$	1.316	0.650	10.638	1.299	0.624	10.777
	$6_1^+ \to 4_1^+$	1.688	0.840	13.033	1.874	0.932	11.739
	$8_1^+ \to 6_1^+$	1.896	0.945	15.822	1.424	0.710	21.067
	$10_1^+ \to 8_1^+$	1.350	0.674	28.148	–	–	–
	$12_1^+ \to 10_1^+$	2.128	1.062	21.616	–	–	–

[29] at energies $(0; 0^+)$ and $(0.877, 2^+)$ MeV, respectively. The experimental levels 2.176 and 4.050 MeV have been confirmed, but the theoretical spin and parity values (6^+) and (8^+) do not agree with available experimental data. For this nucleus, the experimental scheme of levels has been produced to 5.474 MeV, so the states with energy values $7.278; 10^+$ and $9.406; 12^+$ MeV have been identified as new levels in this study. The state 8^+ assigned for experimental level 5.474 MeV is unassigned for the spin and parity experimentally.

3.2. Reduced electric quadrupole transition probability

The radial wave functions for the single-particle matrix elements have been calculated by using the default Skyrme interaction (Sk20) in NuShellX@MSU code with effective nucleon charges. We also calculated the reduced electric quadrupole transitions by fitting the experimental values. The SK20 parameters are given in Table 2. In Table 3, the comparisons of experimental data with theoretical results

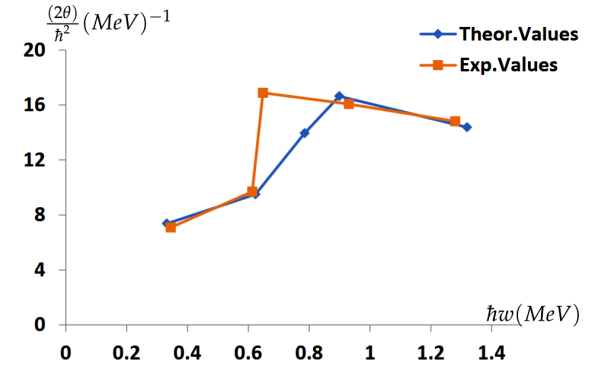

Fig. 1. Inertia moments as a function of the rotational energy for even ^{56}Fe isotope

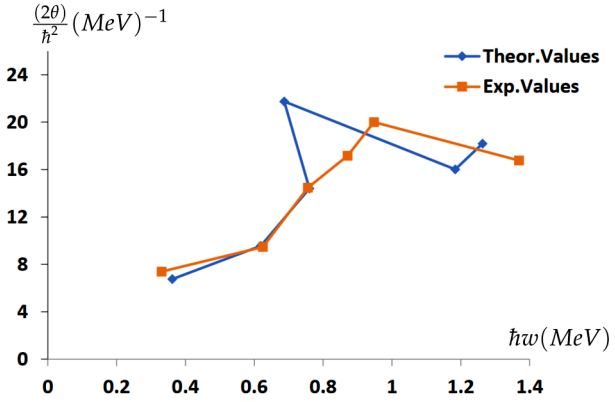

Fig. 2. Inertia moments as a function of the rotational energy for even ^{58}Fe isotope

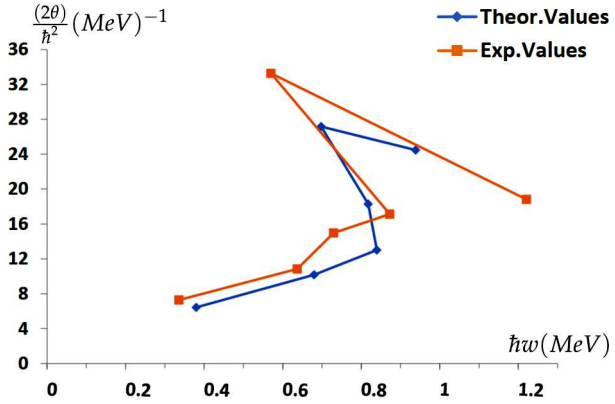

Fig. 3. Inertia moments as a function of the rotational energy for even ^{60}Fe isotope

for the reduced electric quadrupole transition probabilities $BE(2)\downarrow$, deformation parameters β_2, intrinsic quadrupole moments (Q_0) for $^{56-62}$Fe isotopes in the low-lying states are presented, by presenting a

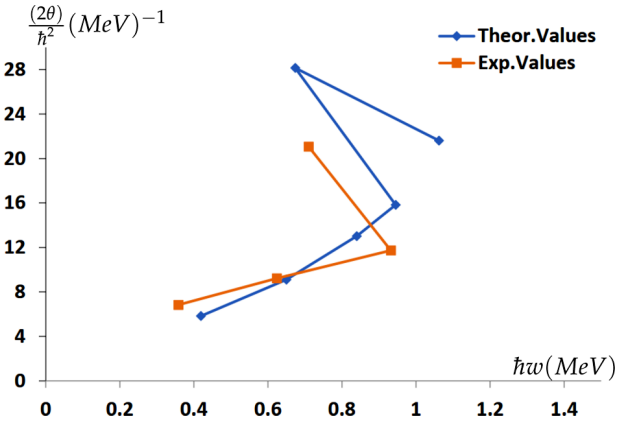

Fig. 4. Inertia moments as a function of the rotational energy for even ^{62}Fe isotope

sighif information on the nuclear structure. We arrive at the excellent agreement between the calculated values of the transition strength $B(icantE2\downarrow)$ for most isotopes in this study such as the values of $B(E2\downarrow)$ from $2_1^+ \to 0_1^+$ and $4_1^+ \to 2_1^+$ that are $213.9e^2$ fm^4 and $286.2e^2$ fm^4 for ^{56}Fe nucleus. The $B(E2\downarrow)$ values from $2_1^+ \to 0_1^+$, $6_1^+ \to 4_1^+$, $8_1^+ \to 6_1^+$ are $246.8e^2$ fm^4, $275e^2$ fm^4, $48.85e^2$ fm^4 for ^{58}Fe nucleus. In the case of ^{60}Fe nucleus, $B(E2\downarrow)$ values from $2_1^+ \to 0_1^+$ and $4_1^+ \to 2_1^+$ are $189.9e^2$ fm^4 and $239.5e^2$ fm^4. Finally, $B(E2\downarrow)$ value for $2_1^+ \to 0_1^+$ is $205.6e^2$ fm^4 for ^{62}Fe nucleus. Furthermore, new values of the reduced electric quadrupole transition for these isotopes have been experimentally expected (yet unknown). In these calculations, another fundamental properties of the nuclei have been revealed such as the shapes of nuclei. A lot of nuclei with neutron (N) or proton (Z) numbers far from a magic number generally have deformed shapes. The simplest deformations are quadrupole deformations, where the nuclei can take the oblate, prolate, or spherical shapes. The quadrupole deformed nuclei are classified as prolate $(Q_0 > 0)$ or oblate $(Q_0 < 0)$, but $(Q_0 = 0)$ for spherical nuclei. From Table 3, the calculated quadrupole deformation parameters depend on the reduced electric quadrupole transition $(BE2\uparrow; 0^+ \to 2^+)$. By applying relation (19) from the same table, we have shown that all calculated and experimental values of quadrupole deformation parameters of all nuclei are in the excellent agreement. The intrinsic quadrupole moments of $^{56-62}$Fe nuclei can be calculated by using relation (17). The results of calculations of intrinsic

quadrupole moments are given in Table (3) and agree with the available experimental values. We note that the intrinsic quadrupole moments $Q_0 > 0$, which indicates that these isotopes have prolate shapes.

3.3. Rotational energy and inertia moment

Table 4 displays the comparison between calculated and experimental values of gamma energies, moments of inertia, and rotational energies of $^{56-62}$Fe isotopes. Moments of inertia and rotational energies values in Table 4 have been calculated from relations (22) and (21), respectively. The results of these calculations have an acceptable agreement with available experimental data. To illustrate the nature of the back-bending properties of these nuclei, the relationship between the rotational energies for even numbers of neutrons $N = 30$, 32, 34, and 36 in nuclei and moments of inertia is established. New values have been predicted in these calculations relative to the unknown experimental values. A linear proportionality occurs between moments of inertia and rotational energies in the lowest order as is seen in Figs. 1, 2, 3 and 4 for $^{56-62}$Fe isotopes, respectively. These figures show that the moments of inertia rapidly increase according to $2_1^+ \to 0_1^+$, $6_1^+ \to 4_1^+$, $8_1^+ \to 6_1^+$ for the above isotopes, respectively. Back bending phenomenon appears clearly in Fig. 2, 3, and 4 and shows the location of the back-bending in ^{60}Fe nucleus at $J = 10^+$. As for ^{58}Fe and ^{62}Fe nuclei, the back-bending appears at 8^+ and 10^+, respectively.

4. Conclusions

In this current study, many nuclear properties of $^{56-62}$Fe isotopes such as yrast energy levels, reduced electric quadrupole transition probabilities(BE2), quadrupole deformation parameters (β_2), intrinsic quadrupole moments (Q_0), rotational energies ($\hbar w$), and moments of inertia $\left(\frac{(2\theta)}{\hbar^2}\right)$ have been determined. We indicate that the nuclear shell model with the HO interaction in the HO model space is very successful for explaining these properties. We have got an acceptance agreement of the theoretical results and experimental data on all properties that have been calculated in the present work. We have confirmed and determine the total angular momenta and parities for some experimental energy levels. Some new values of energy levels, reduced electric quadrupole transition probabilities, rotational energies, and inertia moments for $^{56-62}$Fe isotopes have been determined, but the experimental data are not available in some cases till now. Such values would add more information for theoretical knowledge about all isotopes under study. The back bending phenomenon has appeared clearly for ^{60}Fe nucleus at $J = 10^+$ and, for ^{58}Fe and ^{62}Fe nuclei, at 8^+ and 10^+, respectively. All calculations of the above nuclear properties for each nucleus in this study have contributed to reaching the better comprehension of basic concepts of the nuclear structure. The results of this study are of importance for compiling the Nuclear Data Table.

1. J.M. Blatt, V.F. Weisskopf. *Theoretical Nuclear Physics* (Springer, 1979) [ISBN: 13.978-0-486-66827-7].
2. A.K. Hasan, F.H. Obeed, A.N. Rahim. Positive parity levels of ^{21,23}Na isotopes by using the nuclear shell model. *Ukr. J. Phys.* **65** (1), 3 (2020).
3. B.A. Brown, B.H. Wildenthal. Status of the nuclear shell model. *Ann. Rev. Nucl. Part. Sci.* **38**, 29 (1988).
4. F. Brandolini, C.A. Ur. Shell model description of $N \simeq$ $\simeq Z1f7/2$ nuclei. *Phys. Rev. C* **71** (5), 1 (2005).
5. M. Honma, T. Otsuka, B.A. Brown, T. Mizusaki. Effective interaction for pf-shell nuclei. *Phys. Rev. C* **65** (6), 1 (2002).
6. S.N. Liddick, P.F. Mantica, R.V.F. Janssens, R. Broda, B.A. Brown, M.P. Carpenter, B. Fornal, M. Honma, M. Horoi, T. Mizusaki, A.C. Morton, W.F. Mueller, T. Otsuka, J. Pavan, A. Stolz *et al.* Development of new shell structure in pf-shell nuclei. *J. Phys.: Conf. Ser.* **49**, 013 (2006).
7. A. Novoselsky, M.Vallieres, O. Laadan. Full fp shell calculation of ^{51}Ca And ^{51}S. *Phys. Rev. lett.* **79**, (22), 4341 (1997).
8. P.C. Srivastava, I. Mehrotra. Large scale shell model calculations for odd-odd $^{58-62}$Mn isotopes. *Eur. Phys. J. A* **45** (2), 185 (2010).
9. A. Johnson, H. Ryde, J. Sztarkier. Evidence for a singularity in the nuclear rotational band structure. *Phys. Lett. B* **34** (7), 605 (1971).
10. A. Johnson, H. Ryde, S.A. Hjorth. Nuclear moment of inertia at high rotational frequencies. *Nucl. Phys. A* **179** (3), 753 (1972).
11. R.A. Sorensen. Nuclear moment of inertia at high spin. *Rev. Mod. Phys.* **45** (3), 353 (1973).
12. A.M. Shirokov, A.I. Mazur, J.P. Vary, I.A. Mazur. Oscillator basis, scattering and nuclear structure. *J. Phys.: Conf. Ser.* **403**, 012021 (2012).
13. L. Coraggio, A. Covello, A. Gargano, N. Itaco, T.T.S. Kuo. Shell model calculations and realistic effective interactions. *Prog. Part. Nucl. Phys.* **62** (1), 135 (2009).

14. A. Gargano, L. Coraggio, A. Covello, N. Itaco. Realistic shell model calculations and exotic nuclei. *J. Phys.: Conf. Ser.* **527**, 1 (2014).
15. E. Caurier, G.M. Pinedo, F. Nowacki, A. Poves, A.P. Zuker. The shell model as unified view of nuclear structure. *Rev. Mod. Phys.* **77**(2), 427 (2005).
16. B.A. Brown. The nuclear shell model towards the drip lines. *Prog. Part. Nucl. Phys.* **47**(2), 517 (2001).
17. O. Sorlin, M.G. Porque. Nuclear magic numbers: new features far from stability. *Prog. Part. Nucl. Phys.*, **61**(2), 602 (2008).
18. P.J. Brussaard, P.W.M. Glademans. *Shell Model Application in Nuclear Spectroscopy* (North-Holland, 1977) [ISBN-10: 0720403367, ISBN-13: 978-0720403367].
19. F. Ertugral, E. Guliyev, A.A. Kuliev. Quadrupole moments and deformation parameters of the $^{166-180}$Hf, $^{180-186}$W and $^{152-168}$Sm isotopes. *Acta Phys. Pol. A* **2-B** (128), 254 (2015).
20. M. Haberichter, P.H.C. Lau, N.S. Manton. Electromagnetic transition strengths for light nuclei in the skyrme model. *Phys. Rev. C* **93** (3), 1 (2016).
21. B. Pritychenko, M. Birch, B. Singh, M. Horoi. Tables of $E2$ transition probabilities from the first 2^+ states in even-even nuclei. *At. Data Nucl. Data Tables* **107**, 1 (2016).
22. S. Raman, C.W. Nestor, JR., P. Tikkanen. Transition probability, $B(E2)$ from the ground to the first-excited 2^+ state of even-even nuclides. *At. Data Nucl. Data Tables* **78** (1), 1 (2001).
23. S.S.M. Wong. *Introductory Nuclear Physics, Edition No. 2* (Wiley, 1990) [ISBN: 978-0-471-23973-4].
24. I.M. Ahmed, H.Y. Abdullah, S.T. Ahmad, I. Hossain, M.K. Kasmin, M.A. Saeed, N. Ibrahim. The evolution properties of even-even $^{100-110}$Pd nuclei. *Int. J. Mod. Phys. E* **21** (12), 1 (2012).
25. B.A. Brown, W.D.M. Rae.The shell-model code NuShellX@MSU *Nucl. Data Sheets* **120**, 115 (2014).
26. H. Junde, H.Su, Y. Dong. Adopted levels gammas for ^{56}Fe *Nucl. Data Sheets* **112**, 1513 (2011).
27. C.D. Nesaraja, S.D. Geraedts, B.J. Singh. Adopted levels gammas for ^{58}Fe *Nucl. Data Sheets* **111**, 897 (2010).
28. E. Browne, J.K. Tuli. Adopted levels gammas for ^{60}Fe *Nucl. Data Sheets* **114**, 1849 (2013).
29. A.L. Nichols, B. Singh, J.K. Tuli. Adopted levels gammas for ^{62}Fe *Nucl. Data Sheets*, **113**, 973 (2012).

Received 10.02.20

Ф.Х. Обід

РОЗРАХУНОК ВЛАСТИВОСТЕЙ ЯДЕР ДЛЯ ІЗОТОПІВ $^{56-62}$Fe У МОДЕЛЬНОМУ ПРОСТОРІ ОСЦИЛЯТОРНИХ ФУНКЦІЙ З ВИКОРИСТАННЯМ NuShellX@MSU КОДА

В рамках оболонкової моделі розраховано ірастові рівні енергії, ймовірність квадрупольного переходу (BE2), параметр деформації β_2, енергію обертання ($\hbar w$) і момент інерції ($2\theta/\hbar^2$) для смуги основного стану. Програмний код NuShellX@MSU застосовано для визначення властивостей ядер ізотопів $^{56-62}$Fe в модельному просторі осциляторних гармонік (harmonic oscillator, HO) для $P(1f_{7/2})$, $N(2p_{3/2})$, $N(1f_{5/2})$, і $N(2p_{1/2})$ орбіталей і (HO) взаємодії. Результати добре узгоджуються з експериментальними даними. Розрахунки пояснили ефект зворотного вигину для ядер ^{58,60,62}Fe. Визначено і підтверджено спіни і парності рівнів. У розрахунках також визначено інші властивості ядер, для яких наразі немає експериментальних даних.

Ключові слова: ірастові рівні енергії, ймовірність квадрупольного переходу, NuShellX@MSU код, параметр деформації, частота обертання, момент інерції.